The Universal Behavior of striped patterns

BIRS, Kelowna, July '22

and

ENS, Lyon, September '22

- The order parameter equation is a gradient flow with energy determined by metric and curvature 2-forms of phase surface
- Defects with topological indices integer multiples of $1, \frac{1}{2}, \frac{1}{3}$ are solutions. ---- pattern quarks and leptons.

Stripe Patterns

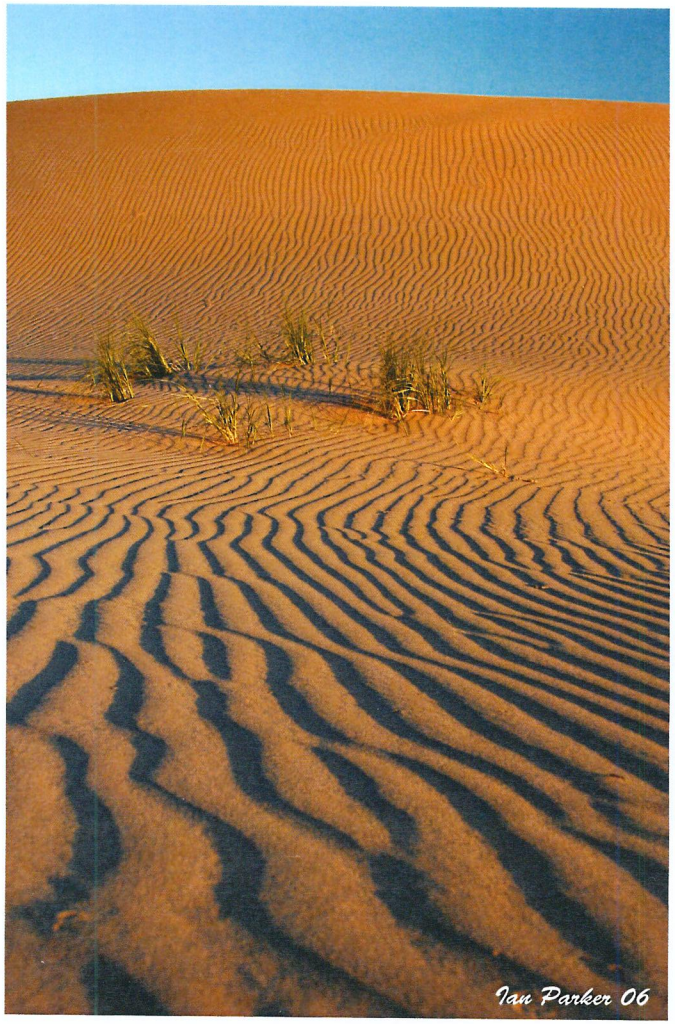

Hexagons (and Stripes)

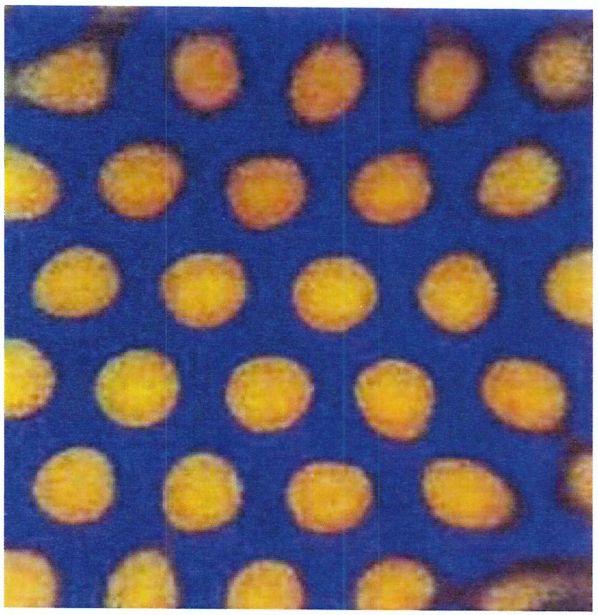

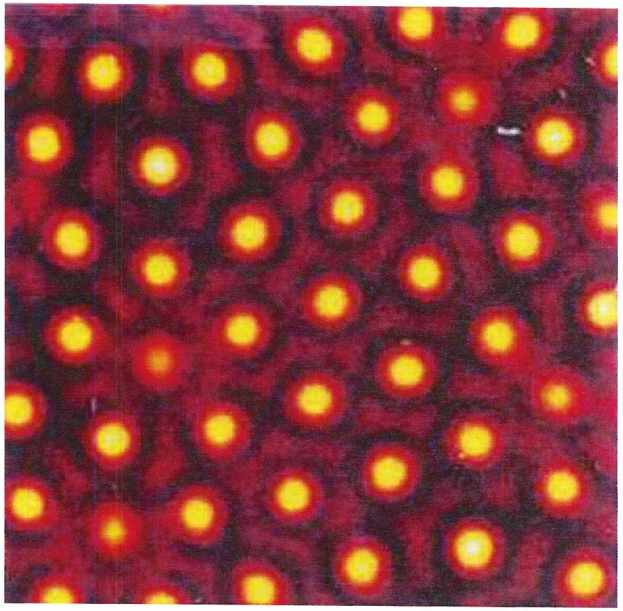

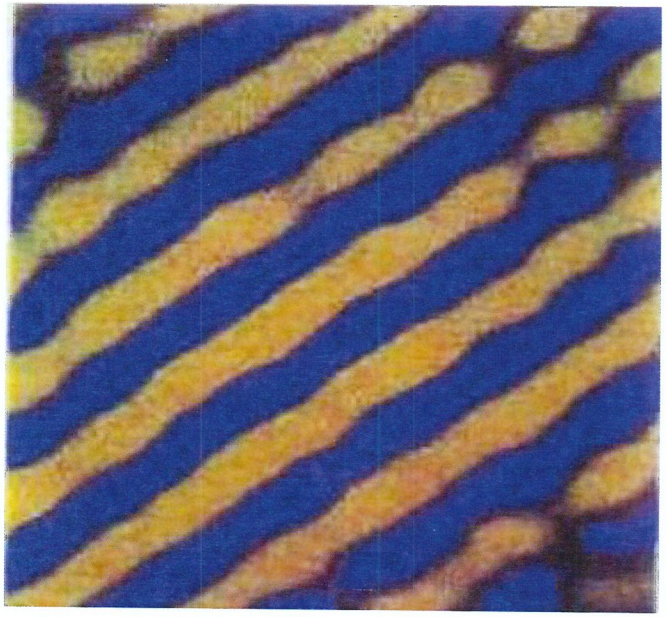

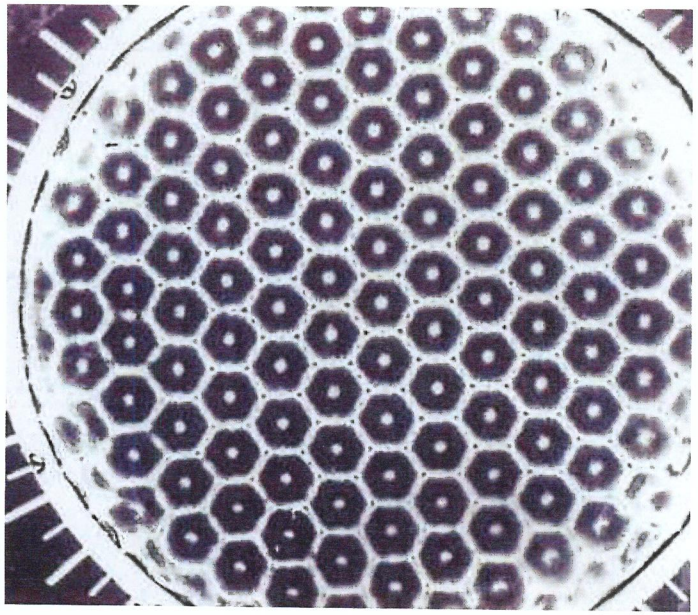

Convection Patterns

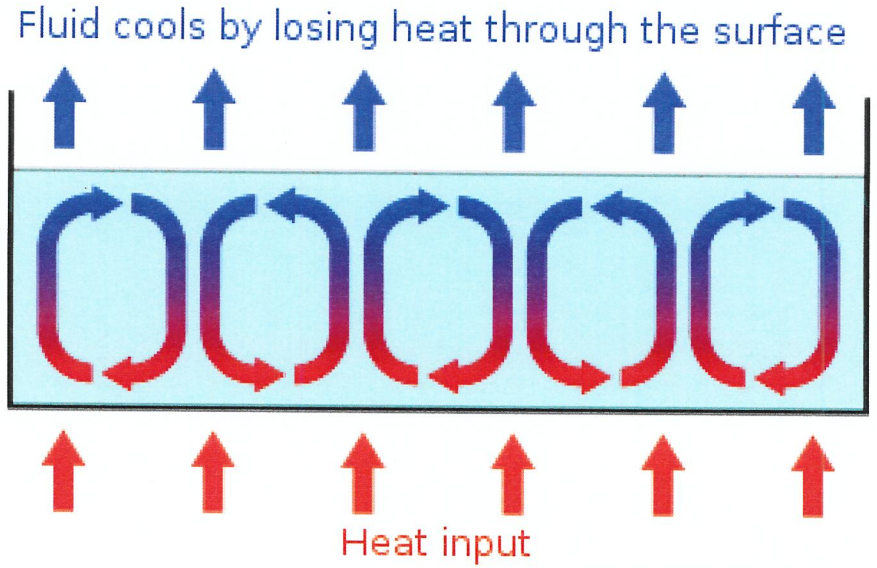

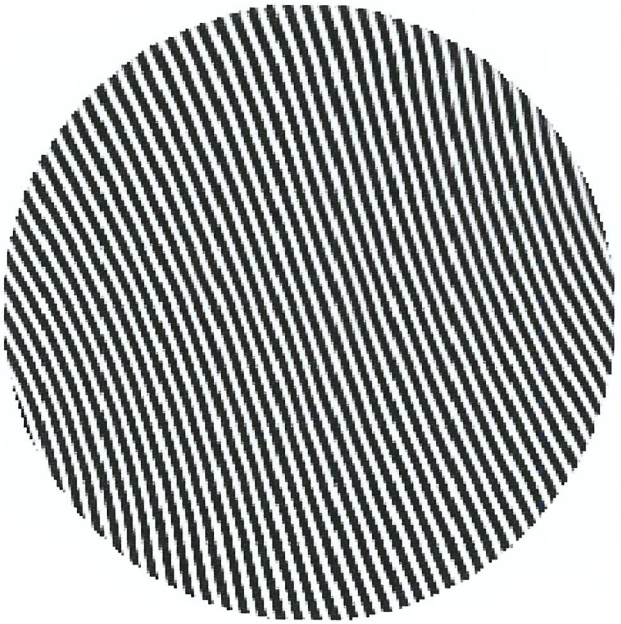

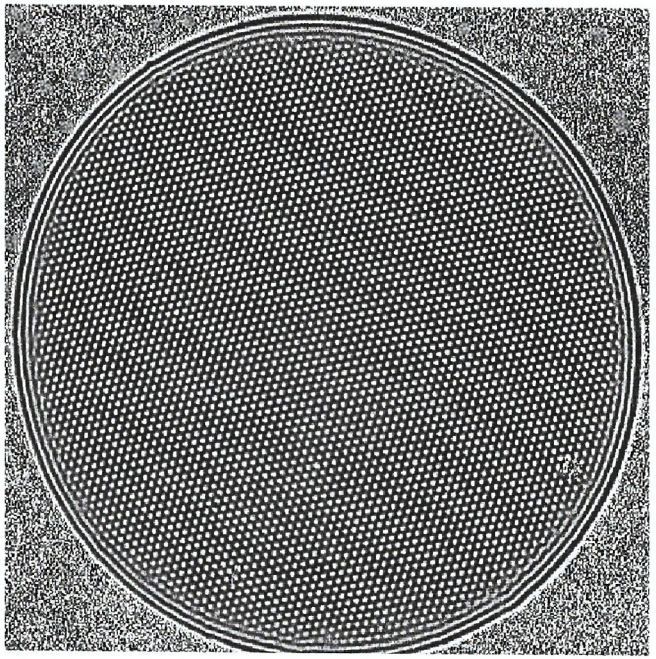

Defects

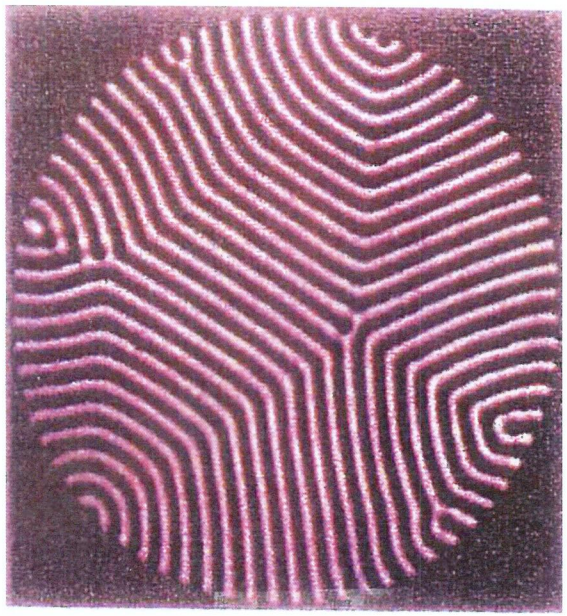

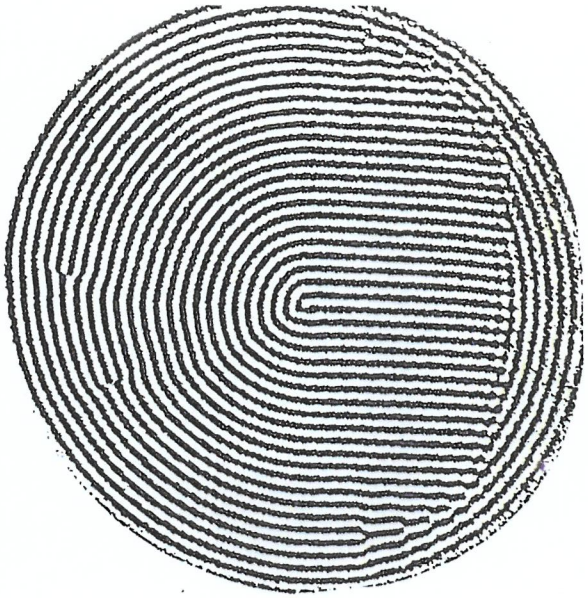

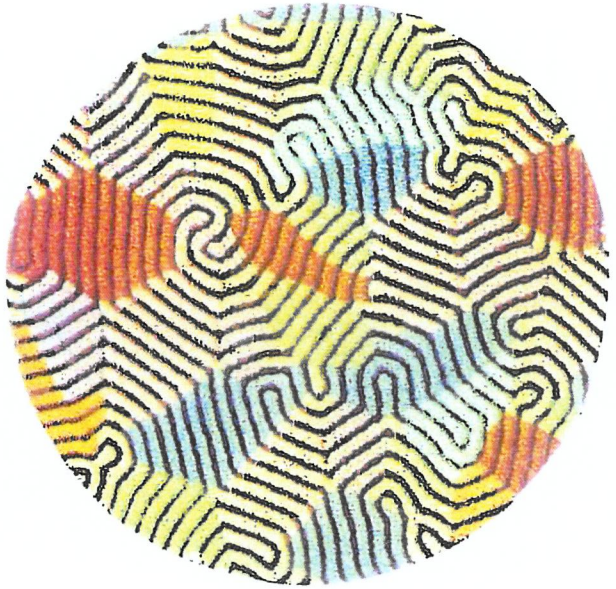

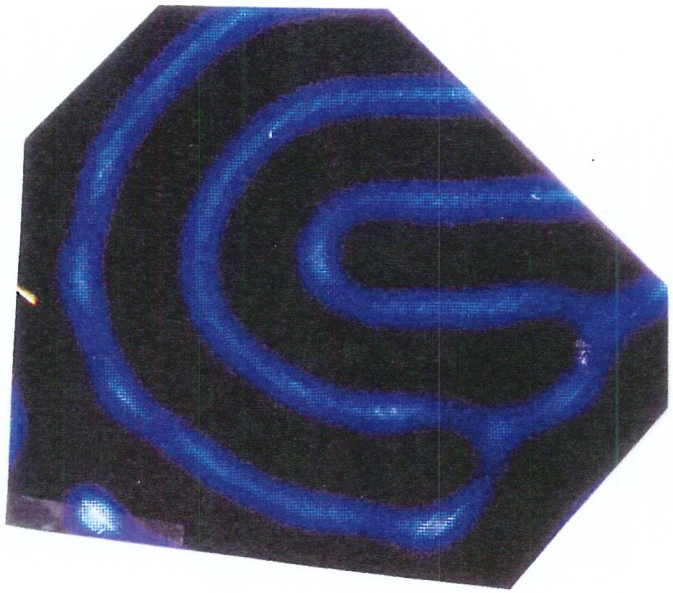

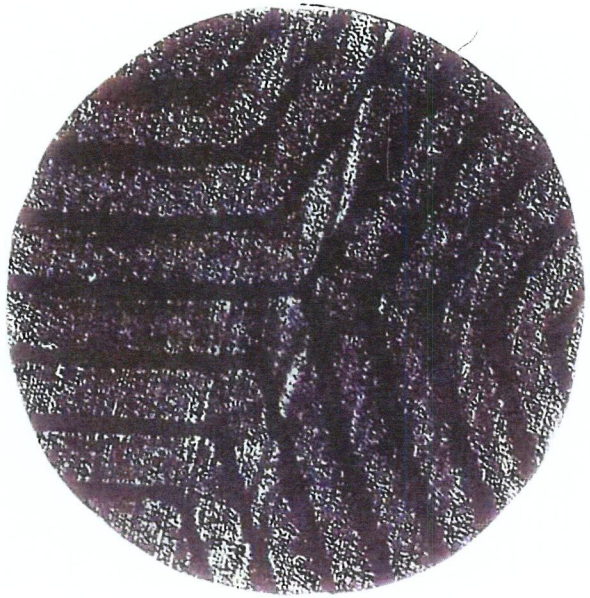

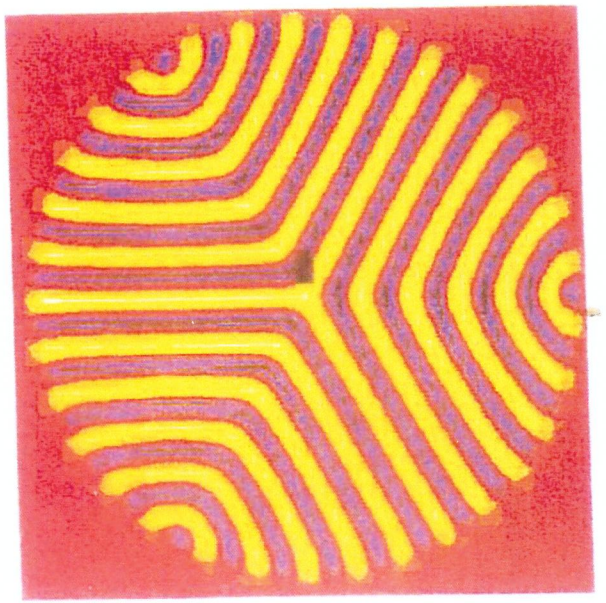

P1*

Pattern (macroscopic) ORDER PARAMETERS $\boxed{\theta,\ \vec{k} = \nabla\theta}$

$\omega \equiv 0 \xrightarrow{R > R_c}$ instability $\qquad \omega = f(\theta)$; $\nabla\theta = \vec{k}$

f: 2π-periodic

$\vec{k}$: changes on macroscopic scale

breaks continuous translational symmetry

but not rotational symmetry

Defects (canonical V, X) + composites (VV, XX, VX, VXXX)

+ phase grain boundaries (PGBs)

Topological indices:

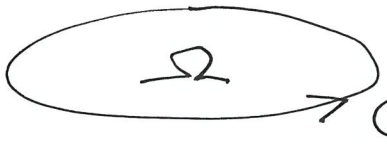

$$2\int_\Omega (f_x g_y - f_y g_x)\, d\vec{x} = k_B^2 \int_C d\varphi = k_B^2\, T$$

$f_x g_y - f_y g_x \propto$ Gaussian curvature of θ

twist

$T(V) = -\pi$

$T(X) = \pi$

$$\int_\Omega (\nabla \times \vec{k})\, d\vec{x} = \int_C \vec{k}\cdot d\vec{x} = [\theta]_C$$

$\nabla \times \vec{k}$ = wavevector vorticity

Circulation

Defects

(a)
CONCAVE DISCLINATION
V
(b)
CONVEX
X
(c)
SADDLE
V V
(d)
TARGET
XX
(e)
V-X pair
"HANDLE"
(f)
DISLOCATI
XX
VV

(P2*)

Microscopic field $\omega(x, y, \cdots, t)$ obeys

$$\omega_t = -\frac{\delta E}{\delta \omega} \; ; \; \text{e.g. } E = \int \left\{ \frac{1}{2}\left((\nabla^2 + k_0^2)\omega\right)^2 - \frac{1}{2} R\omega^2 + \frac{1}{4}\omega^4 + \frac{\beta}{2}\omega^2(\nabla\omega)^2 + \kappa \right\} d\vec{x}$$

- Exact 2π periodic soln. (stripes / rolls)

$$\omega(x, y, t) = f\left(\theta; \{A_n(k^2)\}, R\right\}, \vec{k} = \nabla\theta = \text{const.}\Big) = \sum_{n \text{ odd}} A_n(k^2, R)\cos n\theta$$

if $\omega \to -\omega$ sym.

- Modulated 2π periodic soln; $\varepsilon = \frac{\lambda}{\ell} \ll 1$

$$\omega(x, y, t) = f\left(\theta; \vec{k}\left(\vec{X} = \varepsilon\vec{x}, T = \varepsilon^2 t\right) = \nabla_{\vec{x}}\theta = \nabla_{\vec{X}}\textcircled{M}\right)$$

Away from onset, $R - R_{cr} = O(1)$, amplitudes slaved to "k^2" as in exact soln.

For $R \simeq R_{cr}$, slaving becomes pde (NWS)

(P3*) Evolution of $\theta(\vec{x},t) = \frac{1}{\varepsilon}\,n\left(\vec{X}=\varepsilon\vec{x},\ T=\varepsilon^2 t\right)$

Idea: Average microscopic eqn.

$$\omega_t\,\delta\omega = -\delta E, \quad E = \int W(\omega, \nabla\omega, \nabla^2\omega, \dots)\, d\vec{x}$$

$$\left(\omega = f(\theta);\ \nabla\theta = \vec{k}(\vec{X},T) = \nabla_{\vec{X}}\, n\right)$$

Substitute

$$\nabla_{\vec{x}} \to \vec{k}\,\partial_\theta + \varepsilon\,\nabla_{\vec{X}}$$

$$\nabla_{\vec{x}}^2 \to k^2\partial_\theta^2 + \varepsilon\left(2\vec{k}\cdot\nabla + \nabla\cdot\vec{k}\right)\partial_\theta + \varepsilon^2\nabla_{X^2}$$

and average $\frac{1}{2\pi}\int_0^{2\pi} \dots\, d\theta = \langle \dots \rangle$

$$\langle f_\theta\,\theta_t\, f_\theta\,\delta\theta\rangle = -\delta\bar{E} = -\delta\int \bar{E}_0 + \varepsilon^2\bar{E}_2$$

$O(\varepsilon)$ disappears

To leading order

$$\langle f_\theta^2\rangle\,\theta_t = -\frac{\delta\bar{E}_0}{\delta\theta} = -\int \frac{d\bar{E}_0}{dk^2}\, 2\vec{k}\cdot\nabla\delta\theta$$

integrate by parts

$$\langle f_\theta^2\rangle\,\theta_t + \nabla\cdot\vec{k}\,B(k^2) + \dots = 0$$

$$B(k^2) = -2\,d\bar{E}_0/dk^2$$

Ph*

Macroscopic order parameter eqn. to leading order

$$\langle f_\theta^2 \rangle \theta_t + \nabla_0 \bar{k} B(k^2) + \cdots = 0$$

$$B(k^2) = -2 \frac{d\bar{E}_0}{dk^2} \; ; \text{ e.g. } \bar{E}_0 = -\frac{1}{4}\langle f^4 \rangle - \frac{\beta}{2}\langle f f_\theta^2 \rangle$$

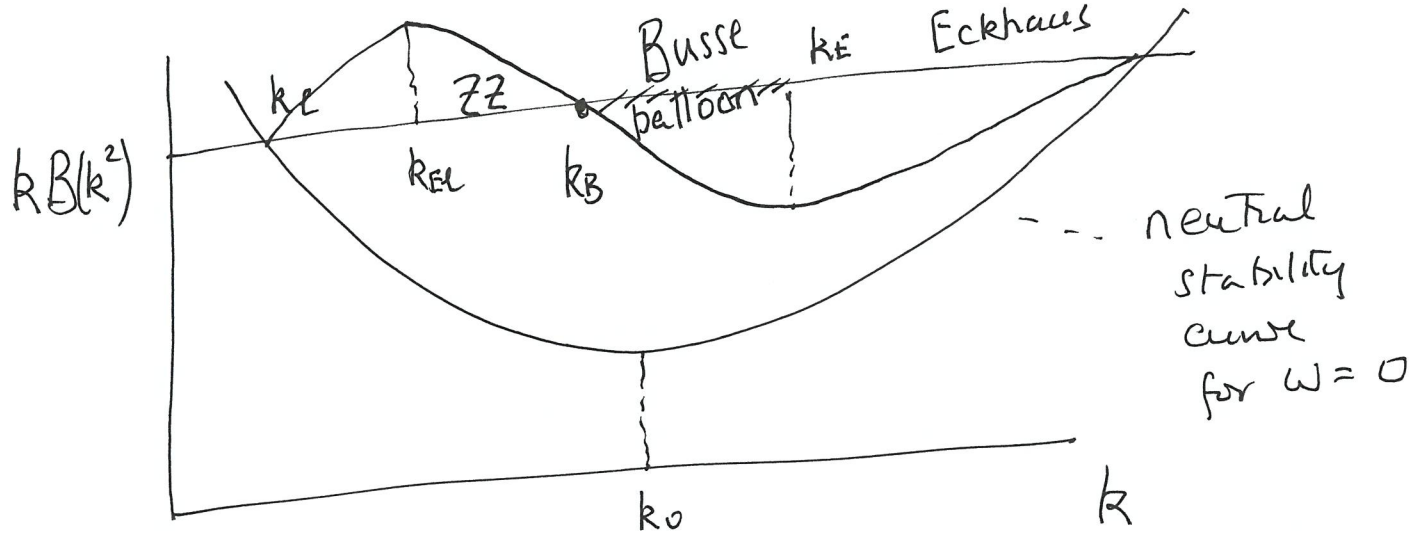

$\nabla . \bar{k} B$ 2nd order quasi linear in θ with

eigenvalues B, $\frac{d}{dk} kB$

viz: $\langle f_\theta^2 \rangle \theta_t + B\theta_{yy} + \frac{d}{dk} kB . \theta_{xx} = 0$

ill-posed for $k < k_B$ or $k > k_E$.

— regularization required.

P5*

$$\langle f_\theta^2 \rangle \theta_t = -\frac{\partial}{\partial \theta} \int \bar{E}_0 + \varepsilon^2 \int \bar{E}_2$$

On horizontal diffusion time scale $T = \varepsilon^2 t = O(1)$, the minimization of $\bar{E}_0$ drives the wavenumber towards its preferred value k_B almost everywhere

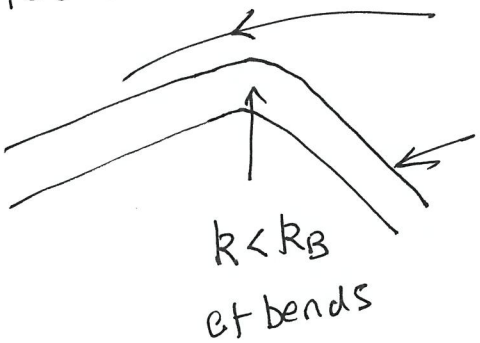

Consequence #1. of $k^2 \to k_B^2$ ac

The original $\bar{E}_1$ and $\bar{E}_2$ are non universal when first averaged but (i) $\bar{E}_1$ is identically zero and (ii) in $\bar{E}_2$, all Terms $\vec{k} \cdot \nabla k^2$ (arising from $k \cdot \nabla A_n(k^2)$) are much smaller than Terms $k^2 \nabla \cdot \vec{k}$. Only remaining

$$\langle f_\theta^2 \rangle_{k_B} \int \left| \nabla \cdot \vec{k} \right|^2 d\vec{x}$$

Pb* Regularized phase diffusion equation

$$\langle f_\theta^2 \rangle \theta_t + \left\{ \begin{array}{l} \nabla \cdot \vec{K} B + \langle f_\theta^2 \rangle \nabla^4 \theta \\ \dfrac{\delta \bar{E}}{\delta \theta} = \dfrac{\delta}{\delta \theta} \left(\int \dfrac{\alpha}{2} G^2 + \dfrac{\eta}{2} (\nabla^2 \theta)^2 \right) \end{array} \right\} = 0$$

$$\alpha = \frac{1}{4 k_B} \left| \left(\frac{dB}{dk} \right)_{k_B} \right| , \quad \frac{\alpha}{2} G^2 = \frac{1}{2} \int_{k^2}^{k_B^2} B \, dk^2 = \overline{E_0}$$

$$\eta = \langle f_\theta^2 \rangle , \quad \beta = \frac{\alpha}{\eta}$$

Solutions of stationary phase diffusion equation

Idea: Reduction to 2 2nd order pde's

Let $\nabla^2 \theta = \beta s G + s \chi \qquad s = \pm 1$

Then $\delta \bar{E} / \delta \theta = 0 \Rightarrow$

$$(**) \quad \nabla^2 \chi + \nabla \left(s \chi \nabla_{\vec{k}} G \right) = -\beta s \nabla_{\vec{k}} \left(\hat{J} \left(\hat{J} - \nabla^2 \theta I \right) \nabla_{\vec{k}} G \right)$$

$$\vec{x} \xrightarrow{\hat{J}} \vec{k} \qquad \hat{J} = \begin{pmatrix} f_x & f_y & \cdots \\ g_x & g_y & \cdots \\ \cdots & \cdots & \cdots \end{pmatrix}$$

P7*

Consequence #2 of $k^2 \to k_B^2$ in any number of spatial dimensions.

Differentiate $k^2 = k_B^2$ w.r.t all spatial variables

$$\Rightarrow \hat{J}\vec{k} = 0$$

Note $\nabla_{\vec{k}} G(k^2) \propto \vec{k}$

$\vec{k}$ is eigenvector of Jacobian $\hat{J}$ with eigenvalue zero.

In 2D $\Rightarrow$ $f_x g_y - f_y g_x \propto$ Gaussian curvature of $\theta(x,y)$

$= 0$.

But GC is conserved density. In $k^2 \to k_B^2$ it is zero.

patches and on phase grain boundaries

It condenses onto points in 2D

and onto loops in 3D

P8*

Linearization of stationary ph. diff. eqn.

(1) $\nabla^2\theta = \beta s G + s\chi$

(2) $\nabla^2\chi + \nabla(s\chi\nabla_{\vec{k}}G) = -\beta s\nabla_{\vec{k}}\left(\hat{J}(\hat{J}-\nabla^2_\theta I)\nabla_{\vec{k}}G\right)$

In 2D, RHS of (2) $= \beta s J \nabla^2_{\vec{k}} G$, $J = \det \hat{J}$

Since a.e. $k^2 \to k_B^2$, $G \simeq (k^2 - k_B^2)$

Hopf-Cole (Forsythe Vol 6; exercise)

$$\theta = \frac{1}{\beta s}\ln\psi \quad , \quad \chi = \psi v$$

$$\begin{cases} \nabla^2\psi - (\beta^2 k_B^2 + \beta\chi)\psi = 0 \\ \nabla^2 v - (\beta^2 k_B^2 + \beta\chi)v = -4\beta\psi^{-1}J. \end{cases}$$

J is local (Dirac delta function).

$J = \det \hat{J}$.

P9*

Self-dual solutions $\mathcal{J} \equiv 0$ I PGB's

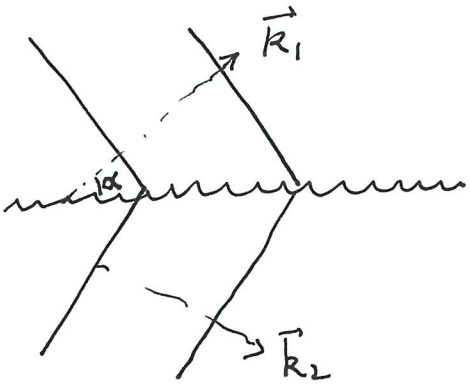

$\vec{k} = \nabla\theta = \frac{1}{2}(\vec{k}_1+\vec{k}_2) + \frac{1}{2}s(\vec{k}_1-\vec{k}_2)\tanh\frac{1}{2}(\vec{k}_1-\vec{k}_2)\cdot\vec{x}$

Energy per unit length $\frac{4}{3}\eta k_B^3 \sin^3\alpha$

unstable when $\alpha \gtrsim 43^\circ$

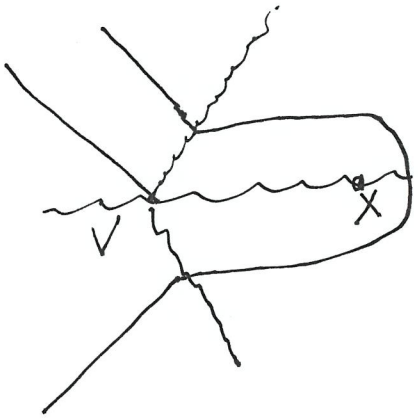

PG with too large a bend spontaneously creates VX pairs

Energy per unit length $\frac{4}{3}\eta k_B^3(1-\sin\alpha)$

II Dislocation (again $\mathcal{J} \equiv 0$).

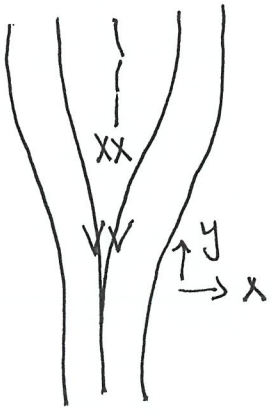

$$\Theta(x,y) = k_B x + \frac{1}{\beta}\ln\left|\frac{1}{2}(1+\exp(\beta\pi\,\mathrm{sgn}\,x)) + \frac{1}{2}(1-\exp(\beta\pi\,\mathrm{sgn}\,x))\,\mathrm{Erf}\sqrt{\beta k_B}\,\frac{y}{\sqrt{x}}\right)$$

---- Amplitudes may become "active" order parameters near core

P10*

Solutions with localized J

V 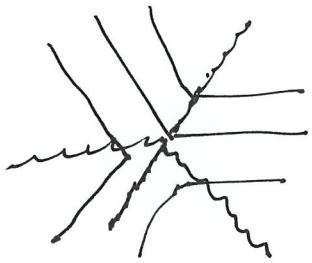 Approx. 3 PGB's

X 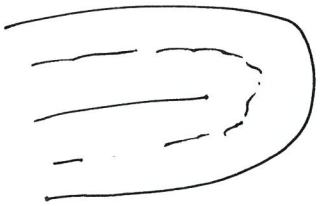

VV, VX, XX (target a vortex)

(Dislocation VV XX

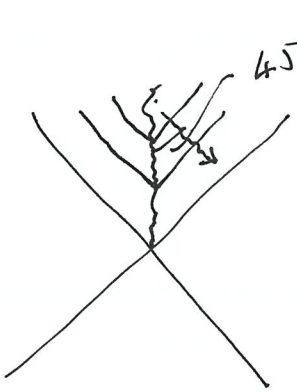

⇒ Separates into 2 V's

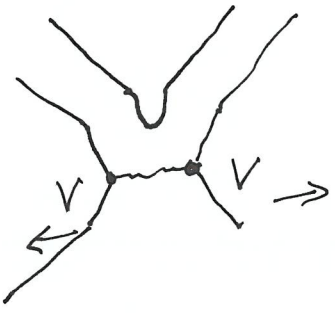

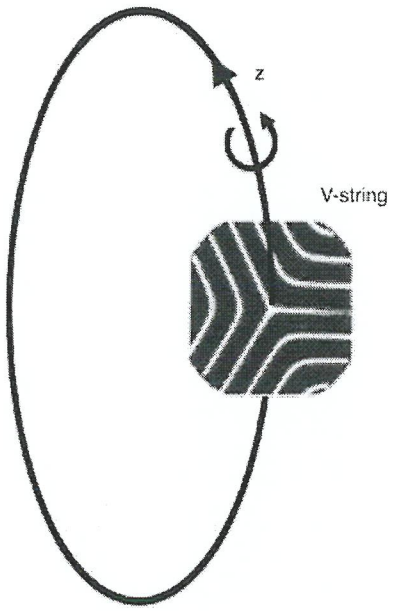

Figure 13: A phase defect in three dimensions with a concave disclination backbone.

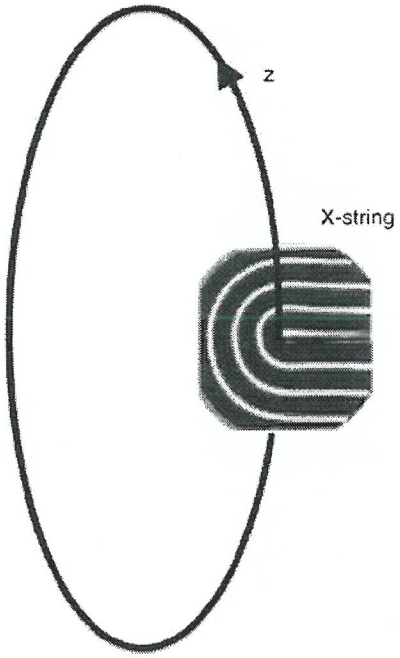

Figure 14: A phase defect with a convex disclination backbone.

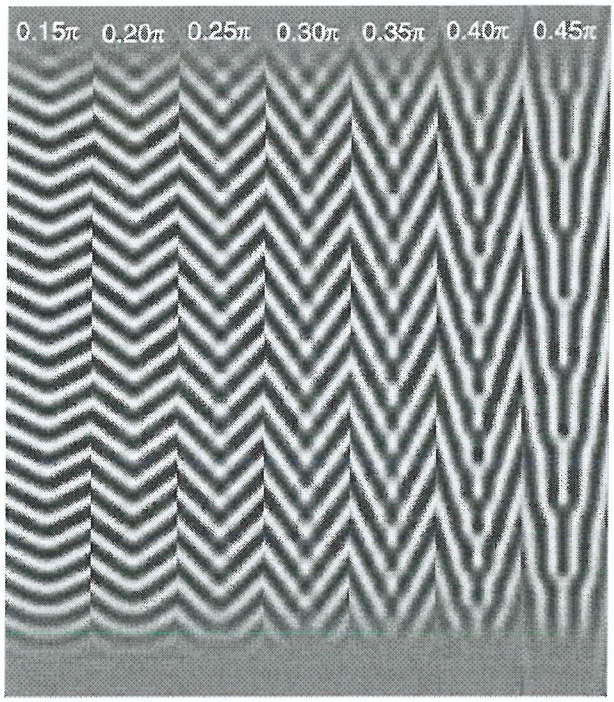

Figure 4: Numerical solutions of the Swift-Hohenberg equation with boundary conditions corresponding to stripes with increasing angles.

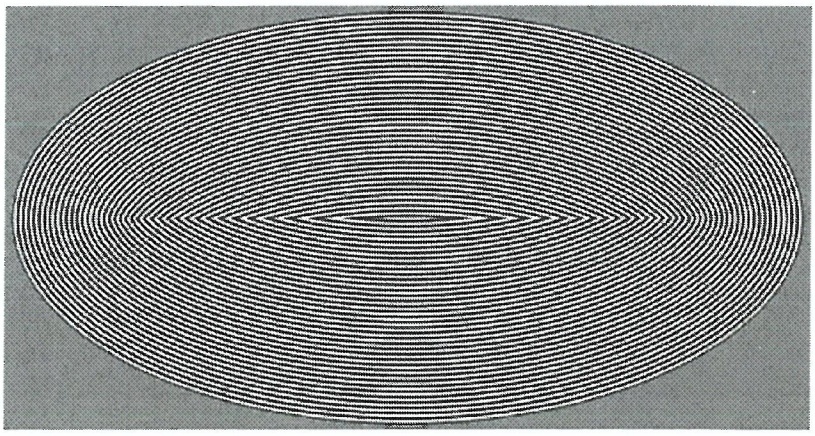

Figure 5: A stripe pattern corresponding to a phase given by the eikonal equation $|\nabla\theta| = 1$.

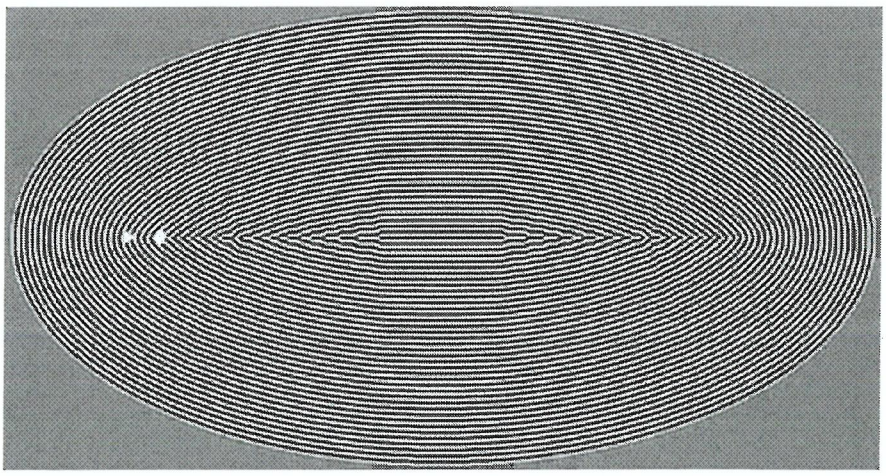

Figure 6: A numerical simulation of the Swift-Hohenberg equation on an elliptical domain. Compare the eikonal solution on the same domain shown in Fig. 5.

boundary normals with phases $0, 2\pi$, etc. marked at intervals of $\frac{2\pi}{k_B}$) regularized by a PGB between the two foci. This would indeed be the solution for an idealized elastic blister whose energy is very similar to (3.2) with carefully controlled boundary conditions. The surface height would rise with constant slope and meet in a ridge located between the two foci where the cavities begin.

However, one observes that the angles at which the phase contours meet the PGB become larger and larger. Figure 6 shows us what happens. The white triangle marks the focus, the center of curvature of the end of the boundary along the major axis. The white diamond marks the point at which the angle reaches its critical value and from that point to the center we see a sequence of dislocations with the contours closest to the major axis parallel to that rather than being shaped as they would if they followed the eikonal solution exactly. But as Fig 7 indicates, the deviation from k_B (here chosen to be unity) is very small and well within the $k - k_B = O(\epsilon)$ tolerance. Fig 8 shows the local energy density which is clearly largest on the sequence of VX pairs near the foci and on the sequence of dislocations nearer the center of the ellipse. Fig. 9 is a repeat of Fig. 6 with a 4:1 aspect ratio with results very close to that of Fig 6. Fig. 10 is the result of a simulation of the Oberbeck-Boussinesq equation at a Prandtl number of 100 (at which the equations are almost but not exactly gradient) and a Rayleigh number of 2000. Figures 11a and 11b are the results of an experiment by Meevasana and Ahlers [9] with ethanol and a simulation of Swift-Hohenberg in an identical geometry. Figures 12a. b are simulations of Swift-Hohenberg.

The challenge is to deduce all this structure from the stationary phase diffusion equation (3.1) for the energy minimizing field. In the far field, away from the major axis between the foci, the Gaussian curvature (Hessian) would appear to be so small as to be negligible so it is likely the self dual approximation obtains. On the outside, the mean curvature is also small so the eikonal solution dominates.

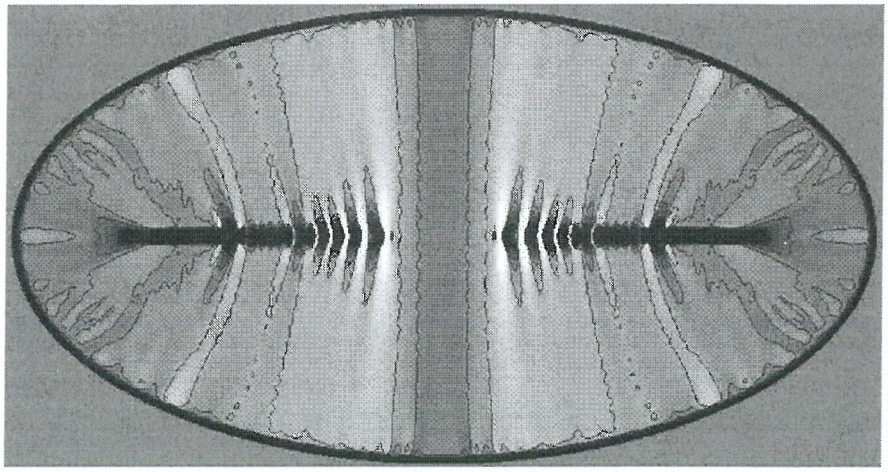

Figure 7: Deviation $|\nabla\theta| - k_B$ of the local wave-number from the preferred wavenumber for the Swift-Hohenberg solution on an elliptical domain.

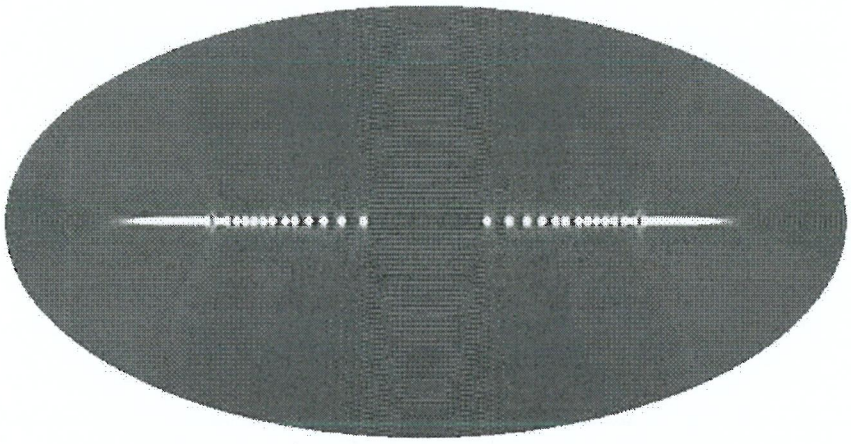

Figure 8: The local energy density on the Swift-Hohenberg solution on an elliptical domain.

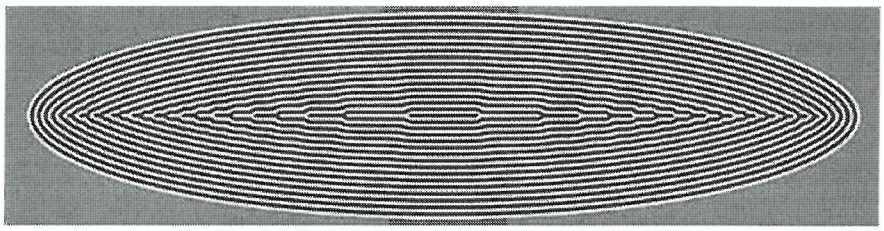

Figure 9: The Swift-Hohenberg solution on an elliptical domain with a larger aspect ratio.

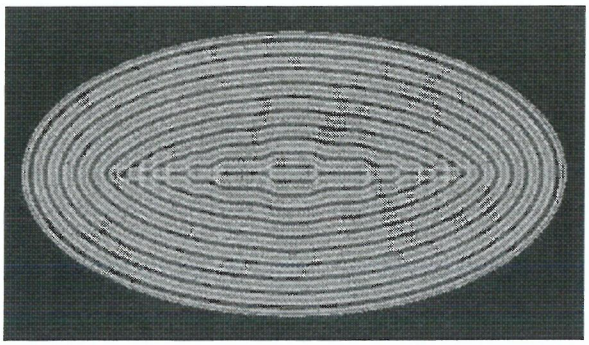

Figure 10: Numerical simulation of the Overbeck-Boussinesq equations for convection.

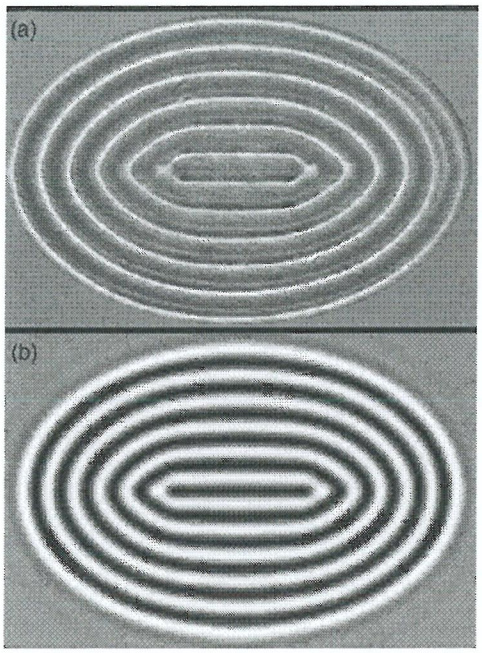

Figure 11: (a) Experimental results for convection in an elliptical container. (b) Simulation of the Swift-Hohenberg equation on the same domain.

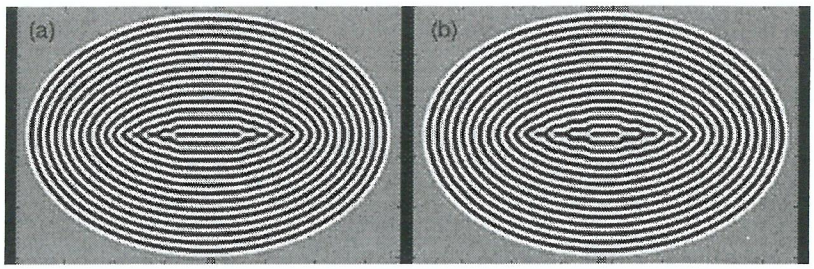

Figure 12: Simulations of the Swift-Hohenberg equation. Note the flattening of the phase contours as the major axis is approached.

But as we move in, the curvature of the phase contours is slightly more pronounced as to allow, if in balance with the strain energy, proportional to $(k^2 - k_B^2)^2$, small deviations in the latter in which $k > k_B$ but well within the Busse balloon and still of order ϵ. Therefore the self dual approximation will allow for some flattening of phase contours as the major axis is approached. Most of the energy in the pattern, as is clear from Fig. 8, resides along the major axis. This behavior can be approximated by a series of phase contours where $\theta = 0$ and gaps where $\dfrac{\partial \theta}{\partial y} = 0$. Following through with this approach allows us to calculate the optimal placing of the divisions so as to minimize the energy [10]. In all likelihood that will be the multidislocation solution (a sum of (3.14) solutions). Another question to address is whether, at the dislocations, one has to reintroduce the amplitude as an additional order parameter as the local wavevector approaches the neutral stability curve where the amplitude is small. In any event, the matching of what is observed, in experiments and in simulations of both the large Prandtl number Oberbeck-Boussinesq equations and its toy model the Swift-Hohenberg equation, provides a healthy but yet unresolved challenge for the theory.

3.2. Pattern quarks and leptons and a second challenge

We saw in 3.1 that the canonical point defects in two dimensional striped patterns were concave (V) and convex (X) disclinations. Their associated invariants, namely the "Twists", measuring the amount of Gaussian curvature condensed onto the point defects, when divided by 2π were fractional, $-\dfrac{1}{2}$ and $\dfrac{1}{2}$ respectively. In three dimensions, the point defect analogues of the V and X will easily dissociate, while loop defects are stable and encode interesting topology [11]. The defects that are structurally stable are loops (see Figures 13 and 14) in which the cross sections are concave and convex disclinations.

As we shall see, they still retain their "spin" or $\pm\dfrac{1}{2}$ invariants. However because the tori which envelope these loops have two independent closed loops on their surfaces on which the amount of twists of the $\vec{k}$ director are invariant, each loop defect has an additional invariant which in the case of the V (X) string or loop with a concave (convex) disclination cross-section, can be integer multiples of $\dfrac{1}{3}$ (1). Because of the analogy with "charge" we call these objects pattern quarks and leptons.

Plant Patterns (Fibonacci)

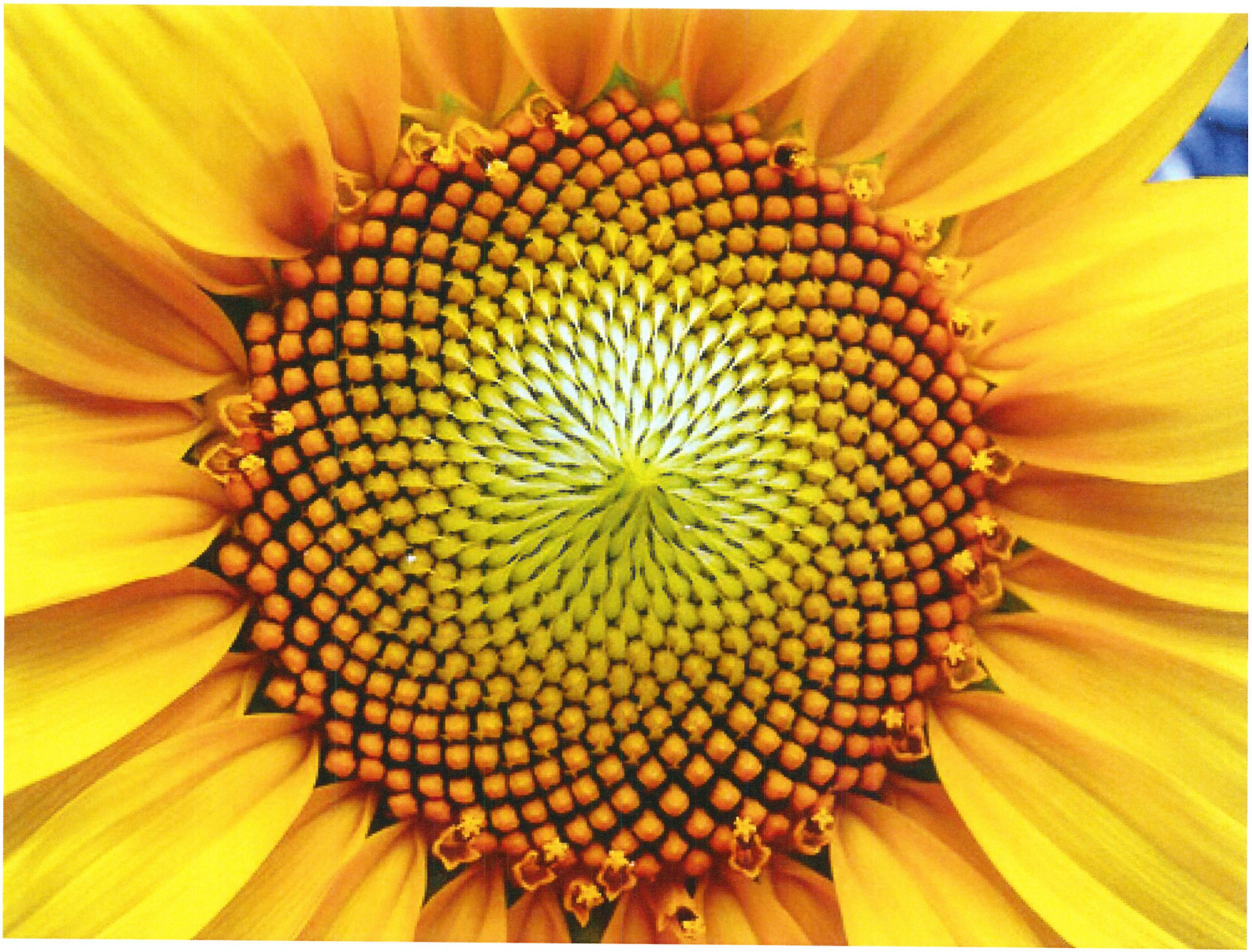

Convection and Megalithic Art